NAVAL POSTGRADUATE SCHOOL
Monterey, California

THESIS

A NUMERICAL STUDY OF EDDY INTERACTIONS WITH A BAROTROPIC OCEANIC JET

by

George P. Davis, Jr.

June 1988

Thesis Advisor D.C. Smith, IV

REPORT DOCUMENTATION PAGE

1a REPORT SECURITY CLASSIFICATION UNCLASSIFIED	1b RESTRICTIVE MARKINGS
2a SECURITY CLASSIFICATION AUTHORITY	3 DISTRIBUTION / AVAILABILITY OF REPORT Approved for public release, distribution is unlimited
2b DECLASSIFICATION / DOWNGRADING SCHEDULE	
4 PERFORMING ORGANIZATION REPORT NUMBER(S)	5 MONITORING ORGANIZATION REPORT NUMBER(S)
6a NAME OF PERFORMING ORGANIZATION Naval Postgraduate School 6b OFFICE SYMBOL (*If applicable*) 68	7a NAME OF MONITORING ORGANIZATION Naval Postgraduate School
6c. ADDRESS (*City, State, and ZIP Code*) Monterey, California 93943-5000	7b. ADDRESS (*City, State, and ZIP Code*) Monterey, CA 93943-5000
8a. NAME OF FUNDING / SPONSORING ORGANIZATION 8b OFFICE SYMBOL (*If applicable*)	9. PROCUREMENT INSTRUMENT IDENTIFICATION NUMBER
8c. ADDRESS (*City, State, and ZIP Code*)	10 SOURCE OF FUNDING NUMBERS PROGRAM ELEMENT NO. / PROJECT NO / TASK NO / WORK UNIT ACCESSION NO.

11 TITLE (*Include Security Classification*)

A NUMERICAL STUDY OF EDDY INTERACTIONS WITH A BAROTROPIC OCEANIC JET

12. PERSONAL AUTHOR(S)
Davis, Jr., George P.

13a. TYPE OF REPORT	13b TIME COVERED	14. DATE OF REPORT (*Year, Month, Day*)	15 PAGE COUNT
Master's Thesis	FROM _____ TO _____	1988 June	64

16 SUPPLEMENTARY NOTATION
The views expressed in this thesis are those of the author and do not reflect the policy or position of the Dept. of Defense or the U.S. Navy.

17 COSATI CODES			18 SUBJECT TERMS (*Continue on reverse if necessary and identify by block number*)
FIELD	GROUP	SUB-GROUP	Gulf Stream, Gulf Stream Vortices, Numerical Simulations

19 ABSTRACT (*Continue on reverse if necessary and identify by block number*)

Mesoscale vortices generated by western boundary currents are well observed and documented, particularly in the case of the Gulf Stream System. The movement of these rings in the region of the Gulf Stream is well studied and has been ascribed to the following physical mechanisms: (1) the beta effect on an isolated ring, (2) advection of a ring in a recirculation regime, (3) downstream advection of a ring in contact with a jet, and (4) vorticity advection associated with the jet and eddy interaction.

Utilizing a two layer, nonlinear primitive equation model, an examination of eddy movement is conducted, with focus on eddy/jet interaction. A series of numerical experiments is performed in which the initial separation distance between eddy and jet is varied. The model demonstrates that vortex movement is strongly related to the proximity of the vortex to the jet. It also is demonstrated that observed movement is not solely dependent on the beta effect nor on advection due to recirculation.

20 DISTRIBUTION / AVAILABILITY OF ABSTRACT ☒ UNCLASSIFIED/UNLIMITED ☐ SAME AS RPT ☐ DTIC USERS	21. ABSTRACT SECURITY CLASSIFICATION
22a NAME OF RESPONSIBLE INDIVIDUAL D.C. Smith, IV	22b TELEPHONE (*Include Area Code*) (408) 646-3350 22c. OFFICE SYMBOL 68Si

DD FORM 1473, 84 MAR 83 APR edition may be used until exhausted
All other editions are obsolete

SECURITY CLASSIFICATION OF THIS PAGE

*U.S. Government Printing Office: 1986–607-047

Approved for public release; distribution is unlimited.

A Numerical Study of Eddy Interactions with a Barotropic Oceanic Jet

by

George P. Davis, Jr.
Lieutenant, United States Navy
B.S., United States Naval Academy, 1981

Submitted in partial fulfillment of the
requirements for the degree of

MASTER OF SCIENCE IN METEOROLOGY AND OCEANOGRAPHY

from the

NAVAL POSTGRADUATE SCHOOL
June 1988

ABSTRACT

Mesoscale vortices generated by western boundary currents are well observed and documented, particularly in the case of the Gulf Stream System. The movement of these rings in the region of the Gulf Stream is well studied and has been ascribed to the following physical mechanisms: (1) the beta effect on an isolated ring, (2) advection of a ring in a recirculation regime, (3) downstream advection of a ring in contact with a jet, and (4) vorticity advection associated with the jet and eddy interaction.

Utilizing a two layer, nonlinear primitive equation model, an examination of eddy movement is conducted, with focus on eddy/jet interaction. A series of numerical experiments is performed in which the initial separation distance between eddy and jet is varied. The model demonstrates that vortex movement is strongly related to the proximity of the vortex to the jet. It also is demonstrated that observed movement is not solely dependent on the beta effect nor on advection due to recirculation.

TABLE OF CONTENTS

LIST OF TABLES

LIST OF FIGURES

I. INTRODUCTION

A. THE GULF STREAM SYSTEM

The Gulf Stream System is an extensively studied current system due both to its unique dynamical properties as well as to the wealth of accumulated data. It is the strongest current system of the North Atlantic subtropical gyre. Iselin (1936) proposed terminology for a Gulf Stream System subdivided into three distinctly different currents that is commonly accepted and will be used in this study. The first current, the Florida Current, is the portion of the Gulf Stream System that originates in the Gulf of Mexico with the waters that flow through the Yucatan Channel. It passes through the Florida Straits and travels northward along the eastern United States to the vicinity of Cape Hatteras. At this juncture it turns eastward and leaves the continental slope region towards deeper waters. Here it is known as the Gulf Stream as it flows towards the Grand Banks region. It is within this region that the stream develops its characteristic meanders, vortex shedding and ring generation capabilities (Robinson, 1971). The less defined and broader current beyond the Grand Banks is then known as the North Atlantic Current. Figure 1.1 is a schematic summarization of the near surface currents as well as prominent topographic features as presented by Watts (1983).

Typical current velocities of the Gulf Stream between Cape Hatteras and the Grand Banks (hereafter referred to as the Gulf

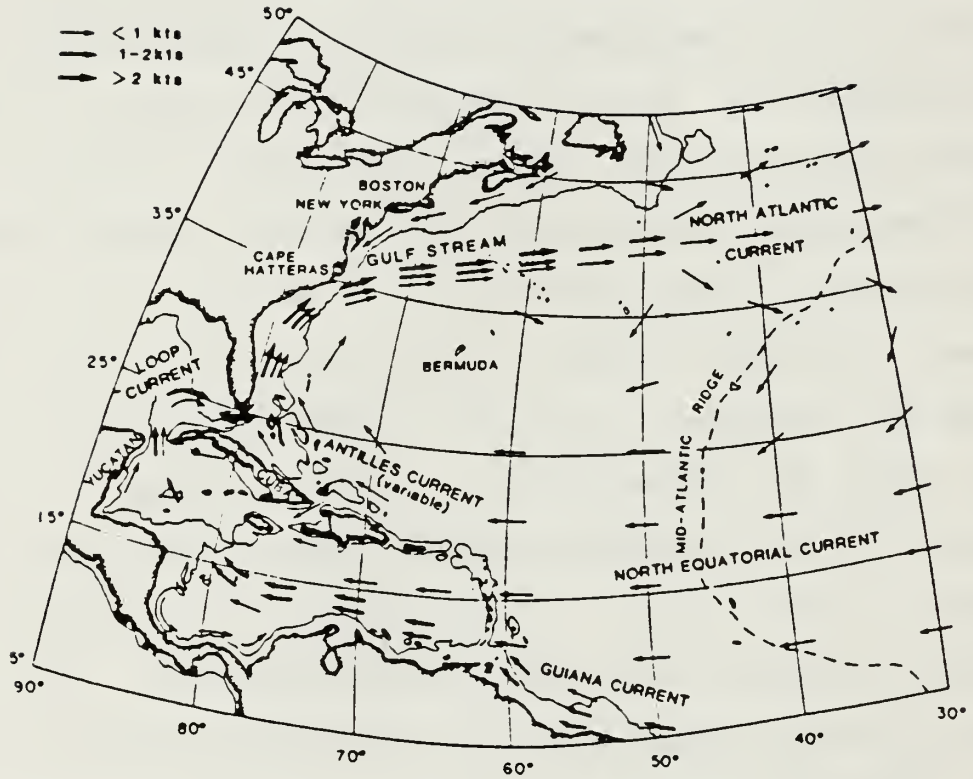

Figure 1.1 Schematic Representation of Western North Atlantic Surface Currents (from Watts, 1983)

Stream) are on the order of 1-2 knots. The dynamics of this area of the Gulf Stream System are being simulated and analyzed in this study.

B. FORMATION OF EDDIES IN THE GULF STREAM

The presence of rings associated with the Gulf Stream has been documented and studied as early as 1793 by Jonathan Williams, grand nephew of Benjamin Franklin (Richardson, 1983). Advancement in techniques of their location, tracking, and documentation as well as advances in the physical understanding of their dynamics have led to several theories concerning their formation. These theories include dynamic instabilities (barotropic and baroclinic) of the Stream and topographic forcing.

The rings associated with the Gulf Stream have either a warm or cold core. A cold core ring is formed by Gulf Stream meanders looping to the south of the stream as depicted in Figure 1.2 (Richardson, 1983, as adapted from Fuglister, 1972). The stems of the meander merge, trapping a core of slope water originally located to the north of the Stream (Fuglister, 1972) in a cyclonic ring. Similarly, warm core rings form anticyclones to the north of the jet in the slope water regions and have as a core, waters entrapped from the Sargasso Sea.

Size and distribution of these rings vary both spatially and temporally. Figure 1.3 gives a synoptic distribution as presented by Richardson, et al., (1978). Depicted is the 15°C isothermal surface. Contours are based on expendable bathythermograph, CTD hydrographic, and satellite infrared data from March 16 until July 9, 1975. Notable

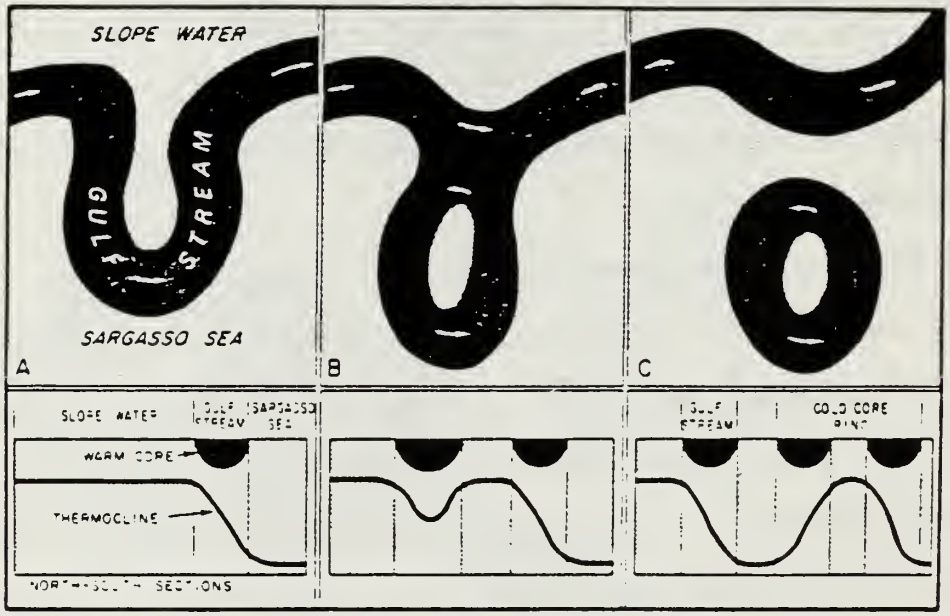

Figure 1.2 Formation of a Cold Core Ring.

Cold core ring forcing as a closed segment of the streamy circulating around a mass of slope water (adapted from Fuglister, 1972, by Richardson, 1983).

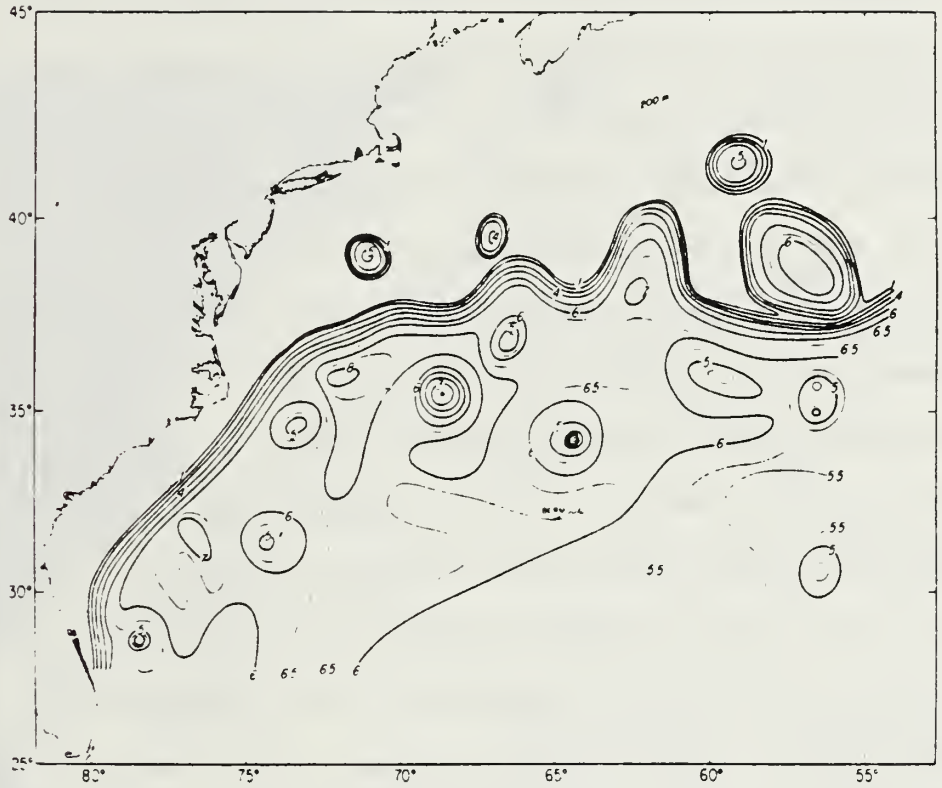

Figure 1.3 Gulf Stream Ring Distribution

Distribution of rings from March 16 to July 9, 1975 as represented by the 15°C isotherm. Primary contour intervals are 100 m and are represented by the darker contour lines (from Richardson, et al., 1978).

in this view is the fact that though the radii of these rings vary, they are of comparable width to the Gulf Stream itself. It is on the basis of these observations that the experimental parameters of this study are based.

C. PROPAGATION CHARACTERISTICS OF RINGS WITHIN THE GULF STREAM SYSTEM

Theories for the movement of rings within the Gulf Stream System vary, with numerous recent studies shedding additional light on these propagation mechanisms. Observationally, the movement of rings is known to vary depending on ring location relative to the Gulf Stream as well as to prominent topographic features such as the New England Seamounts and the continental slope and shelf. While topographic steering may be of importance near the shelf and slope, the primary emphasis of the numerical analysis of this study is instead on the ring and Gulf Stream interactions away from topography.

Rings that are in contact with the stream tend to move downstream at speeds of up to 75 cm/s (Richardson, 1980). Rings that are not in contact with the stream tend to propagate with a westward tendency (varying from northwest to southwest) with typical speeds of 5 cm/s (Lai and Richardson, 1977). Additionally, cyclonic rings may have multiple interactions with the Gulf Stream and their propagation will evolve from eastward when attached to the stream, to southward as the ring is detached from the stream, then westward, and followed by northward and eastward as the ring again interacts with the stream (Richardson, 1980). Additional observations by Fuglister (1977) confirm this "clockwise" propagation scheme for cyclonic eddies.

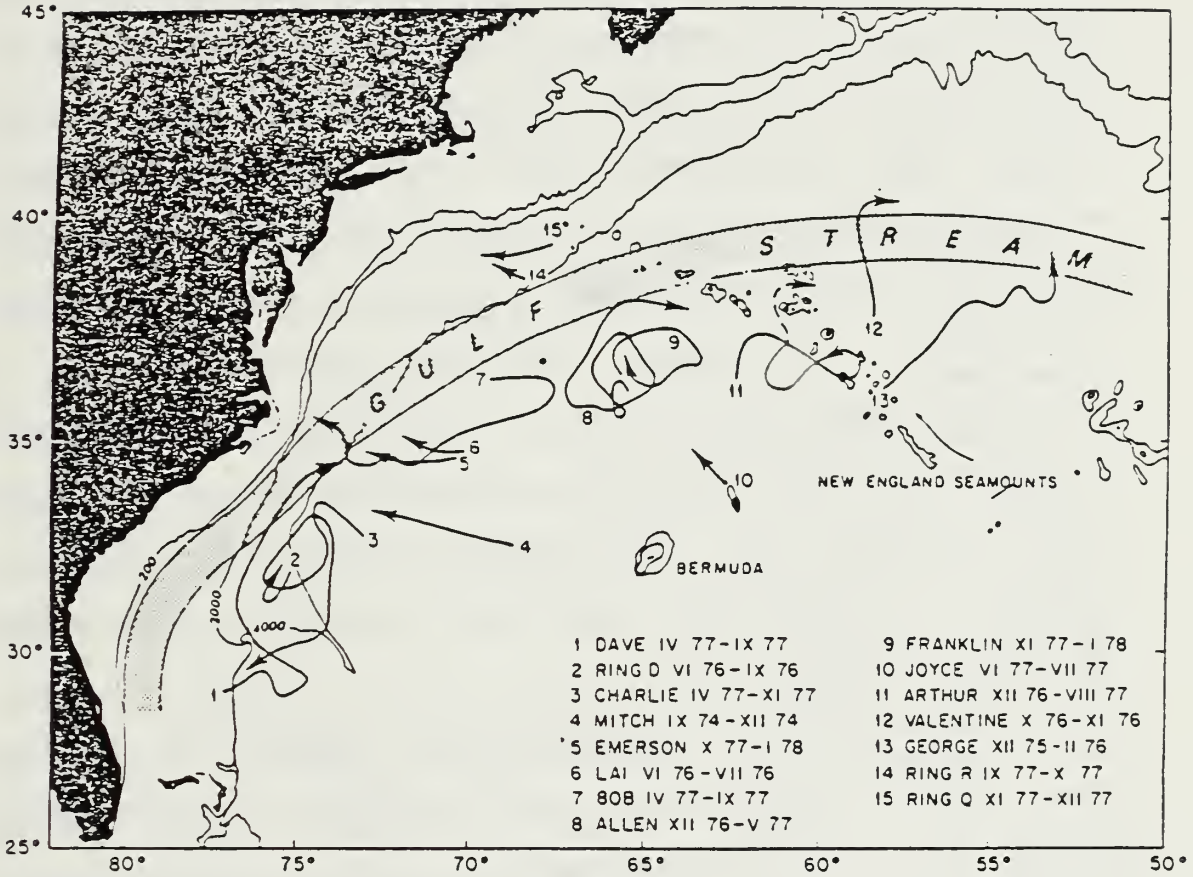

Figure 1.4 Gulf Stream Ring Trajectories

The trajectories of all rings continuously tracked with free-drifting buoys plus one (ring 4) tracked by SOFAR floats (see Cheney et al., 1976). The mean path of the Gulf Stream is shown by shading (from Richardson, 1980).

Figure 1.4 provides results from various cruises and studies that illustrate each of the propagation characteristics provided above.

There have been different mechanisms proposed for ring movement. The first is due to the representation of a vortex as the superposition of many Rossby waves (Mied and Lindemann, 1979). Associated with this beta dispersion-induced westward propagation is a subsequent meridional component of propagation proportional to the strength of the nonlinear terms (Firing and Beardsley, 1976). In this nonlinear case, the gradient in the eastern portion of the eddy is strengthened through differential westward propagation of Rossby waves allowing for northward (southward) propagation components of cyclones (anticyclones). In addition, rings are thought to move due to advection by large scale mean flows. Westward movement is attributed to advection by the 5 cm/s recirculation regime of the Gulf Stream System (Richardson, 1983), while eastward movement is attributed to advection by the Gulf Stream itself when the eddy is attached to with the stream (Richardson, 1980).

An additional theory has been recently suggested by Stern and Flierl (1987). They represent a Gulf Stream ring by a point vortex and the jet by a jump discontinuity in vorticity. Their results, obtained on an f plane, give westward propagation for anticyclones (cyclones) on the north (south) side of the jet. The interaction of an anticyclone (cyclone) with the cyclonic (anticyclonic) side of the jet leads to mutual advection westward, much the same as the interaction of point vortices of opposite sign. The argument for this tendency is linear for eddies adjacent to (but not in the immediate

vicinity of) the jet. They give an analytic solution for eddy propagation speed which is inversely proportional to eddy and jet separation distance. For eddies close to the jet, nonlinear effects become important and eddy propagation speeds are found by using the method of quasigeostrophic contour dynamics.

D. PURPOSE OF THIS STUDY

The primary objectives of this study are the numerical analysis and determination of ring propagation mechanisms as associated with a high velocity oceanic jet. These are determined from numerical experiments in which the initial spatial separation of the jet and ring in relation to each other is varied. Results are obtained using a two layer, nonlinear, primitive equation model. Experimental analyses are made using both cyclonic and anticyclonic vortices on both the north and south sides of an eastward flowing jet. Both beta and f plane simulations are examined. While cyclones to the north of the jet and anticyclones to the south are obviously not naturally occurring phenomena in the general sense, they are nonetheless included for the study and understanding of the dynamics of the problem at hand. Results are compared to observed, analytical and numerical propagation tendencies. The results support specifically a theory of westward propagation tendencies related to vorticity advection due to the nonlinear effects associated with the shear at the jet and ring interface, as well as propagation due to azimuthal perturbations of the ring due again to nonlinear interaction between the jet and ring. The results also show enhanced propagation due to beta and nonlinear effects on isolated vortices.

Complete understanding of the propagation mechanisms and characteristics of the mesoscale vortices associated with the Gulf Stream is necessary for a more thorough understanding of the general circulation of the ocean in its entirety and for the real time prediction of eddy location and movement for operational use in the USN. The latter is due to the extreme acoustic properties associated with the warm and cold core rings.

II. NUMERICAL TECHNIQUES AND MODEL PARAMETERS

A. THE NUMERICAL MODEL

1. Model Equations

Simulation of the Gulf Stream is accomplished utilizing a two layer, primitive equation, semi-implicit, numerical scheme. This model has been used in numerous ocean and mesoscale circulation studies including Hurlburt and Thompson (1980, 1982), Smith and O'Brien (1983), and Smith (1986). The semi-implicit model was initially developed by Smith and O'Brien (1983). Linear test cases were performed as in Smith and Reid (1982) that compared favorably with linear analytic solutions for verification of Rossby dispersion characteristics of the model.

Motion in each layer of the model is governed by a momentum equation:

$$\frac{\partial V_i}{\partial t} + (\nabla \cdot V_i + V_i \cdot \nabla)\, V_i + kxfV_i = -h_i \nabla P_i + A_h \nabla^2 V_i \qquad (2.1)$$

and a continuity equation:

$$\frac{\partial h_i}{\partial t} + \nabla \cdot V_i = 0 \qquad (2.2)$$

with i representing layer index (i=1 upper and i=2 lower). All variables and notation are found in Table 1. The fluid is Boussinesq and hydrostatic and the density in each layer is constant.

2. Model Domain

A rectangular finite difference gridded domain is used in this model with grid resolution ($2\Delta x$) of 20 km. The grid is oriented in

TABLE 1

REFERENCE STATE MODEL PARAMETERS

PARAMETER	SYMBOL	VALUE
E-W Basin Extent	L_y	1100 km
N-S Basin Extent	L_x	800 km
Initial Upper Layer Thickness	h_1	1000 m
Initial Lower Layer Thickness	$h_2(x,y)$	4000 m
Maximum Basin Depth	$(h_1 + h_2)_{max}$	5000 m
Depth of Bottom	$D(x,y)$	5000 m
Coriolis Parameter (@40° N lat.)	f_o	0.94×10^{-4} s^{-1}
df/dy	β_o	2.0×10^{-11} $m^{-1}s^{-1}$
Gravitational Acceleration	g	9.8 m s^{-2}
Reduced Gravitational Acc.	g′	$g\frac{\rho_2-\rho_1}{\rho_1}$
Horizontal Eddy Viscosity Coef.	A_h	100 m^2 s^{-1}
Time Step	Δt	4200 s
Jet Maximum, i th Layer	V_{ij}	100 cms^{-1}
Eddy Maximum, i th Layer	V_{ie}	100 cms^{-1}
Jet Position	L_j	variable
Eddy Position	L_e	variable
Gradient Operator	∇	$\frac{\partial}{\partial x} + \frac{\partial}{\partial y}$
Laplacian Operator	∇^2	$\frac{\partial^2}{\partial x^2} + \frac{\partial^2}{\partial y^2}$
Pressure in Upper Layer	p_1	$g(h_1 + h_2)$
Pressure in Lower Layer	p_2	$p_1 - g^1h_1$

the east-west direction. The domain encompasses 1100 km in the x (east-west) direction and 800 km in the y (north-south) direction. The upper layer of the model extends to 1000 meters while the lower extends from this depth to 5000 meters. No bottom topography is included.

3. Boundary Conditions

Using the orientation above, free slip boundaries are used on both the northern and southern boundaries with no flow normal to the boundaries. The western (upstream) boundary consists of a prescribed inflow velocity, equal in both the upper and lower layers. The eastern (downstream) boundary utilizes a radiation condition (Carmerlengo and O'Brien, 1980), in which flow is advected out of the basin at speed $\Delta x/\Delta t$ when detected adjacent to the boundary. In addition, a frictional absorption layer is implemented on this boundary in which the Laplacian lateral friction coefficient (A_h) in the governing equations is increased from 250 m^2s^{-1} (utilized elsewhere throughout the domain) to 1000 m^2s^{-1} in the final 50 km of the domain along its eastern boundary.

This final condition is obviously not representative of the conditions within the Gulf Stream itself, but is nonetheless utilized in order to prevent back radiation of small scale vorticity disturbances into the active areas of the model domain. Various model simulations showed that the east/west dimension of the domain is extensive in comparison and the dynamics of the jet/ring interactions were not affected by this absorption band.

B. NUMERICAL EXPERIMENTS

1. Reference State

In order to better facilitate the isolation of ring propagation mechanisms, a variety of model simulations and simplifications were made. The first major simplification concerns the stability of the jet itself. The Gulf Stream is both barotropically and baroclinically unstable. The mechanics of its meanders and the continuous variability of its jet axis therefore impose a continuously varying distance between the jet and any existing ring in its vicinity. This in turn imposes additional variables into the propagation mechanisms associated with jet/ring interactions making cross correlation of variables and therefore isolation of specific interactions and propagation mechanisms a somewhat formidable task. Since the intent of this study is the isolation and identification of these propagation mechanisms at and near the jet interface, a barotropically stable jet was used throughout this study. This removes from the problem many potentially complex variables due to jet meandering. It also simplifies the identification of propagation mechanisms and interface processes and provides for the study of these mechanisms based primarily on jet/ring proximity. Accomplishing the identification of the mechanisms in this manner allows for the establishment of a reference data base for future use in more realistic numerical simulations.

The next simplification made in this study is the absence of the southwestward recirculation currents. Various sources and studies list westward ring advection by this flow as a valid propagation

mechanism since the magnitude of the mean return circulation is similar to that of typical ring propagation. Worthington (1976) documents recirculation speeds of 5 cm/s which are similar to the propagation speeds of both cyclonic and anticyclonic rings. In this study, all simulations are conducted without any southwestward mean flow with the intent of identifying other mechanisms that could possibly duplicate observed propagation speeds and directions.

An additional simplification involves the use of an f plane. Experiments are duplicated on both f and beta planes for the further isolation of the propagation mechanisms of the rings. Whereas beta effects are known to produce westward propagation of a ring (Warren, 1967 and Flierl, 1977), an intent of this study is to determine whether other propagation mechanisms are also valid, in particular the point vortex theory as proposed by Stern and Flierl (1987).

Utilizing the aforementioned simplifications the basic state then consists of a two-layer, geostrophically balanced Gaussian jet of the form,

$$h_2(y) = \bar{H}_2 + A_i[1-\exp(-y^2/2L_j^2,)] \tag{2.3}$$

$$h_1(y) = \bar{H}_1$$

with the horizontal scale (L_j) equal to the e-folding width scale of the jet. Additionally, a two-layer, geostrophically balanced, Gaussian vortex is included as represented by,

$$h_2(x,y) = \bar{H}_2 + A[\exp(-R^2/2L^2_e)] \tag{2.4}$$

$$h_1(x,y) = \bar{H}_1$$

with $R^2 = (x^2 + y^2)$ and representing the radial distribution of the ring.

The jet e-folding scale is set at 45 km while the eddy e-folding scale is set at 40 km. Figure 2.1 is the most basic case of the model simulation and exemplifies the stability of the jet from its initial state at day 0 to its final state in the model simulation at day 36. The lines within the figure are lines of constant surface height anomaly and are representative of streamlines of the barotropic current. The increments on the x and y axis of Figure 2.1 and all subsequent model output fields represent 275 and 200 km respectively. Unless otherwise specified the x axis is 1100 km and the y axis is 800 km for all model output fields.

The initial jet and ring velocities are set at 100 cm/s in each layer. In the jet the 100 cm/s velocity is a constant inflow, while that of the ring is a 100 cm/s gradient balanced initial condition based on height anomaly. Figure 2.2 is an example of a model field output of velocity contours showing the comparable velocities in the upper and lower layers.

For the reference state shown previously, and for all subsequent model output field plots the surface height is contoured in centimeters, velocities are contoured in cm/s and potential vorticity in $m^{-1}s^{-1}$.

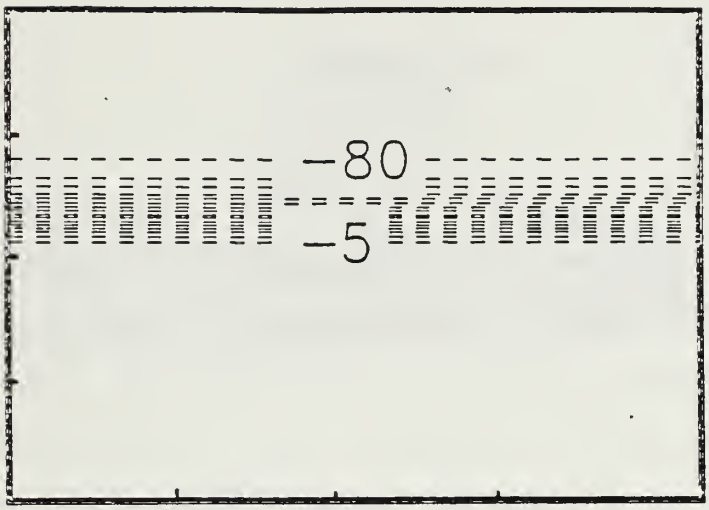

(a)

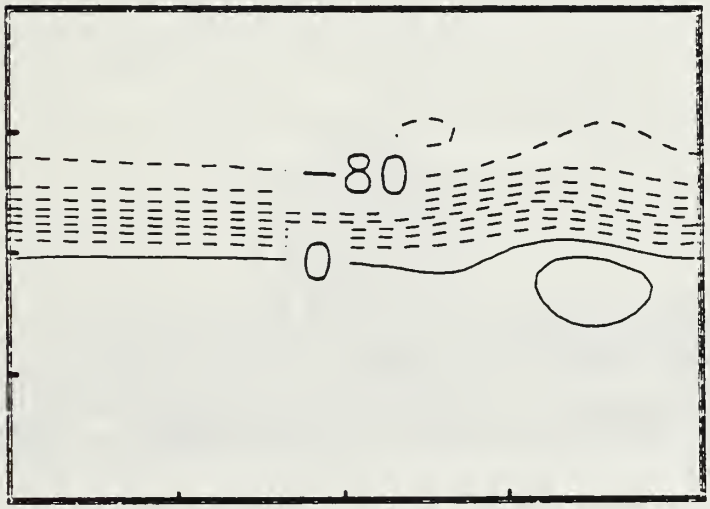

(b)

Figure 2.1 Reference Jet Height Ratio

Height fields at (a) day 0 and (b) day 36. Contours are labeled in centimeters.

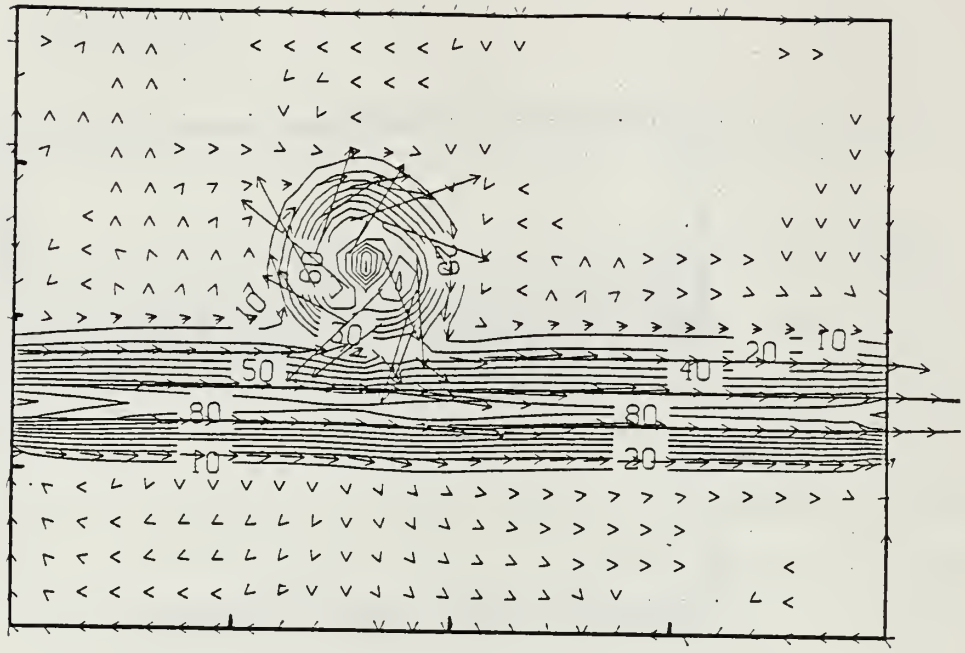

(a)

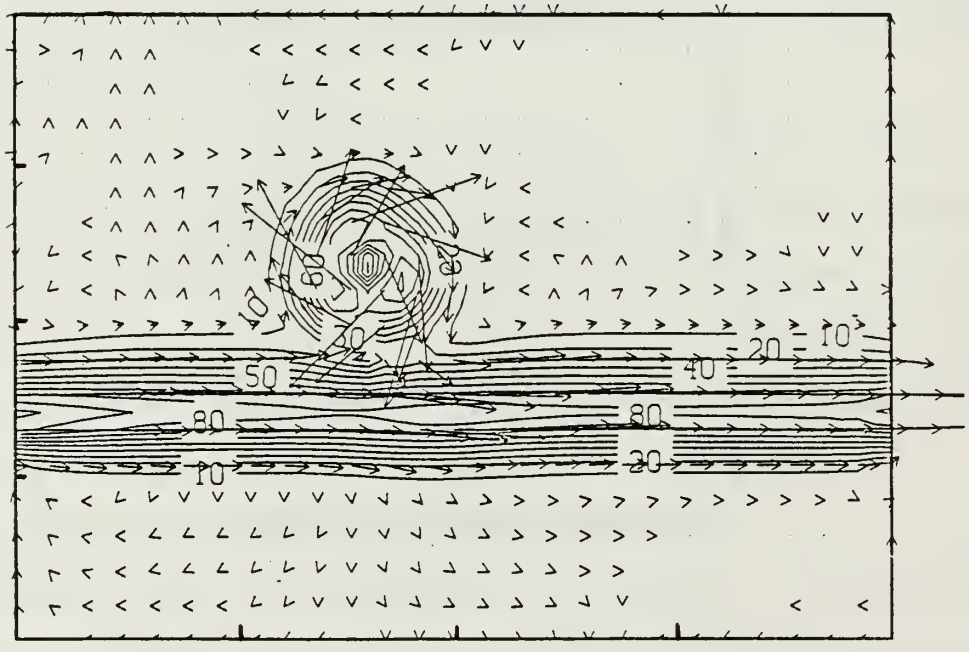

(b)

Figure 2.2 Barotropic Velocity Fields

Velocity fields on day 3 in (a) upper layer and (b) lower layer. Contours are labeled in cm/s.

2. Variation of Parameters

As the focus of this study involves vortex propagation mechanisms due to interaction with the jet interface, the major parameter variation, and indeed the only variable used other than f vs. beta planes, is the vortex and jet locations in the initial state of each model simulation. The major spatial variations utilized are termed "far" and "near" fields. In far field cases, the vortex is initially located at distances farther than 3 jet widths from the jet. In near field cases, the vortex is in the vicinity of the jet (i.e. outer vorticity and height anomaly contours of the jet and vortex intersect). Any other location is termed the "mid" field.

The experiments were divided and subdivided as follows. The first major divisions will be the beta plane and f plane simulations. Within each of these categories fall experiments in which the relative vorticity of the vortex is of the same sense as the vorticity shear of that side of the jet (for example a cyclone located on the north side of the jet). The length of the simulations varies from 21 to 45 days with the vast majority extending to 36 days. A brief description of each experiment follows.

a. Beta Plane Simulations

(1) Experiment Numbers BT1β and BT2β (Initial Beta Plane Experiments). In these experiments an anticyclone and a cyclone with velocity and height anomalies the same as in all other jet inclusive experiments are placed on a beta plane without the presence of a jet. The purpose of this was to determine vortex propagation speeds due solely to westward Rossby wave propagation and nonlinear meridional

effects. This excludes the effects of any possible propagation enhancement or retardation due to the presence of the jet. Initial and final states are given in Figure 2.3.

(2) Experiment Numbers BT3β and BT4β (North Side Anticyclones). An eastward flowing barotropic jet is introduced with an anticyclone to the north of the jet for the purpose of determining jet influences on vortex propagation. Experiment number BT3β is the far field simulation and experiment number BT4β a mid field case. Figure 2.4 shows the height anomaly contours and exhibits the initial conditions of these two cases. Figure 2.4 is also indicative of the initial eddy/jet separation of all other far and mid field experiments.

(3) Experiment Numbers BT5β, and BT6β (North Side Cyclones). The signs of the rings are reversed to cyclones and cases of far and near fields simulated. This near field case was simulated in order to determine if the mutual effects of the jet and ring interactions could actually overcome the northwest propagation tendencies due to nonlinear and beta effects and achieve downstream advection as suggested by Stern and Flierl (1987).

(4) Experiment Numbers BT7β and BT8β (South Side Cyclones). These experiments are as essentially mirror images of experiment numbers BT3β and BT4β with cyclonic rings of an opposite sense placed to the south of the jet with the same eddy jet separation distance. Experiment number BT8β is a far field experiment with experiment number BT7β being a near field case.

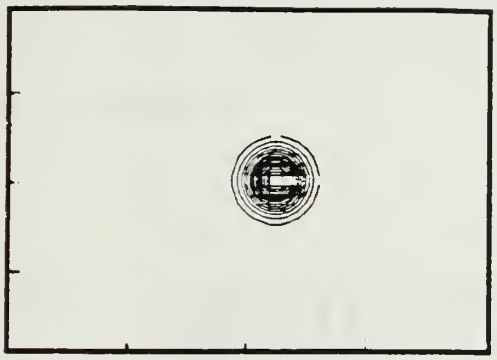

(a) day 0

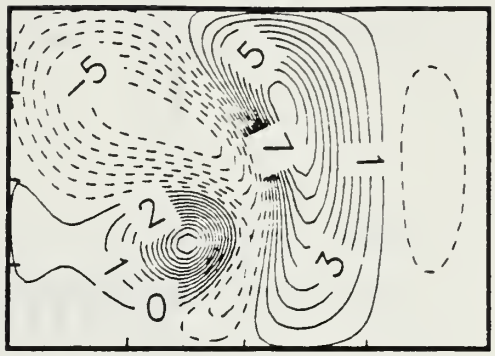

day 36

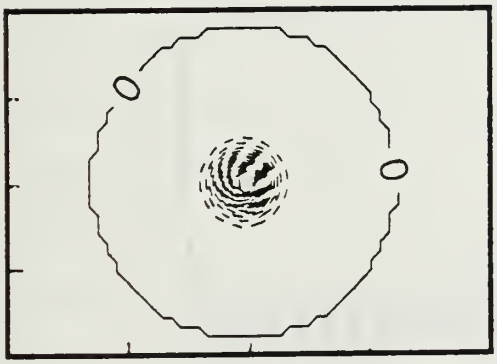

(b) day 0

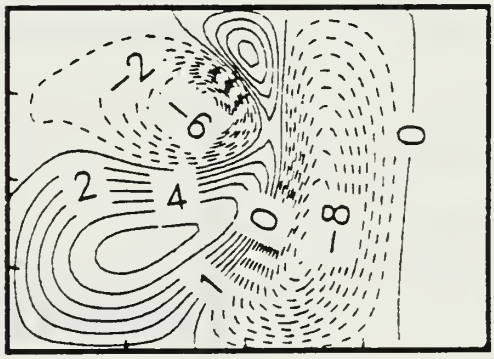

day 36

Figure 2.3 Isolated Eddy Cases

Upper layer height fields for (a) an anticyclonic at day 0 and day 36 and (b) a cyclone at day 0 and day 36.

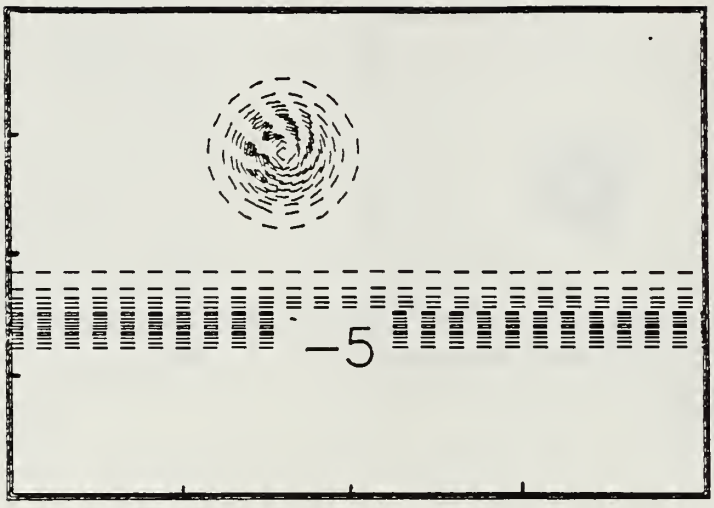

(a)

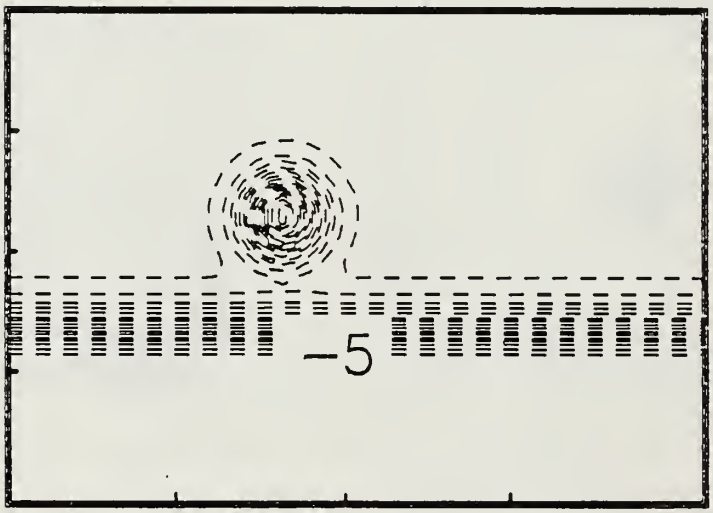

(b)

Figure 2.4 Experiments BT3β and BT4β

Height fields for the initial state of (a) BT3β (far field) and (b) BT4β (mid field)

(5) Experiments Numbers BT9β and BT10β (South Side Anti-cyclones). The rings are reversed in sign from BT7β and BT8β and are a mirrored duplicate of experiment numbers BT5β and BT6β. Experiment BT9β is a mid field case and experiment number BT10β is an extreme near field case.

b. f Plane Simulations

The f plane experiments were conducted with similar initial conditions as that of the beta simulations. These experiments are studied and discussed in greater analytical detail than the beta experiments and are therefore listed in tabular form (Table 2) for a more extensive parameter identification.

Parameter variables listed include initial location L(0) of the eddy relative to the jet edge. Nonlinearity (Q) is quantified as a maximum velocity ratio (V_{max}) to the maximum Rossby wave speed, (βR^2_d). R(0) is a non-dimensional distance between the jet and eddy and is included for direct comparison with the results of Stern and Flierl (1987). Figure 2.5 is a schematic of representative model parameters. Also in this figure "C" and "AC" represent the cyclonic and anticyclonic shear associated with the northern and southern edges of the jet respectively.

TABLE 2

INITIAL CONDITIONS FOR f PLANE EXPERIMENTS

EXP	DIRECTION FROM JET AXIS	EDDY	L(0)	R(0)	Q	MERIDIONAL VEL. (KM/DAY)	ZONAL VEL. (KM/DAY)
BT71F	S	C	60	.9	16	-6.5	-.7
BT71F	N	C	200	2.8	33	-3.1	-1.6
BT70F	N	C	110	1.5	33	2.0	11.9
BT65F	S	AC	120	1.7	33	2.4	11.2
BT66F	S	AC	180	2.5	33	2.8	-1.4
BT28F	S	C	180	2.5	33	-.2	-1.4
BT30F	S	C	160	2.3	33	-.7	-1.4
BT34F	S	C	120	1.7	33	-2.9	-1.4
BT38F	S	C	80	1.1	33	-6.7	-1.2
BT47F	N	AC	120	1.7	33	2.2	-1.3
BT51F	N	AC	160	2.3	33	.84	-1.0
BT55F	N	AC	200	2.8	33	.67	-.9

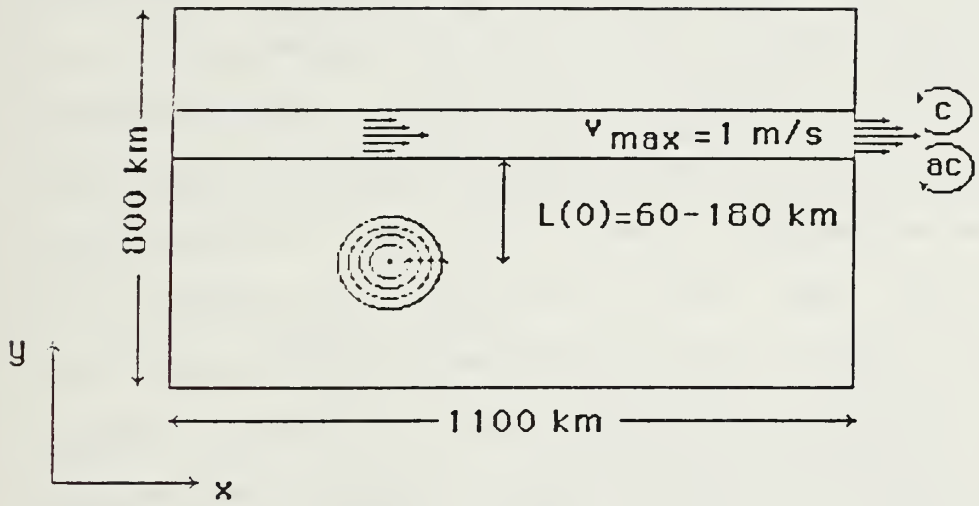

Figure 2.5 Schematic of the Model Domain and Initial Eddy and Jet Configuration

III. RESULTS AND ANALYSIS

A. BETA PLANE EXPERIMENTS

1. Verification of Model Output

Various beta plane experiments were conducted and are discussed first for the purpose of illustrating ring propagation associated with a stable jet in the absence of a recirculation region. The results in this study are compared to previous isolated eddy numerical studies such as that of Mied and Lindemann (1979). In addition, isolated ring propagation is compared to ring propagation in the presence of a jet in order to determine if in fact there is a jet influence on the propagation tendency. The primary purpose here is to determine which "real world" results may be associated with barotropically stable beta plane simulations. With this established, the f plane simulations can then be conducted in order to isolate in detail what additional mechanisms of eddy propagation occur due solely to the jet/eddy interactions. By using this approach, time dependent jet spatial variations due to barotropic and baroclinic instabilities, westward beta propagation and meridional nonlinear self advection, as well as recirculation advection are systematically removed from the equations with only a basic state remaining. Thus only the most rudimentary aspects of jet/ring interactions remain in the f plane model output.

Mied and Lindemann (1979) conducted numerical experiments using a primitive equation, beta plane model of a flat bottom two

layer ocean with a rigid lid imposed. Their experiments were of upper ocean, dispersing and pure barotropic eddies. Their results indicated that westward propagation is associated with beta effects, and with meridional propagation due to nonlinear effects. The rate of meridional and zonal propagation is increased with increasing current strength (i.e. increased nonlinear self advection). This is attributed to the increased advection of planetary vorticity from the north (south) of the eddy to either side of the cyclone (anticyclone). As the strength of the eddy is weakened (numerically through viscous effects) the eddy will tend to turn towards the west. Their results for barotropic eddies indicated that meridional propagation varies from 2.5 to 9 km/day, with zonal rates in the 2 to 3 km/day range. The results of experiment BT1β (Table 3) are not inconsistent with these values.

2. Opposite Sign Cases

Ring trajectories for experiments in which the eddy is of opposite sign as that of the shear vorticity of the jet edge (as in figure 2.5) are shown in Figures 3.1a and 3.1b. These and all other trajectory plots represent 30 days. In 3.1a an isolated anticyclone is included (BT1β) along with a mid and far field case in which a jet is included in the domain to the south of the eddy. Translational velocity averages (in 9 day increments) for each experiment are given in Table 3. In these and all other propagation plots, the jet axis for vortices to the north of the jet is 285 km. For the cases of vortices to the south of the jet, the jet axis is at 555 km.

TABLE 3

TIME AVERAGED BETA PLANE VELOCITIES (NORTH SIDE ANTICYCLONES)

EXPERIMENT	DAY	ZONAL VELOCITY (KM/DAY)	MERIDIONAL VELOCITY (KM/DAY)
BT1β			
	9	-2.0	-3.8
	18	-4.5	-6.0
	27	-1.0	-5.2
BT3β			
	9	-2.4	-4.0
	18	-1.8	-8.3
	27	4.2	-1.6
BT4β			
	9	-2.0	-5.1
	18	.5	-6.0
	27	5.2	3.0

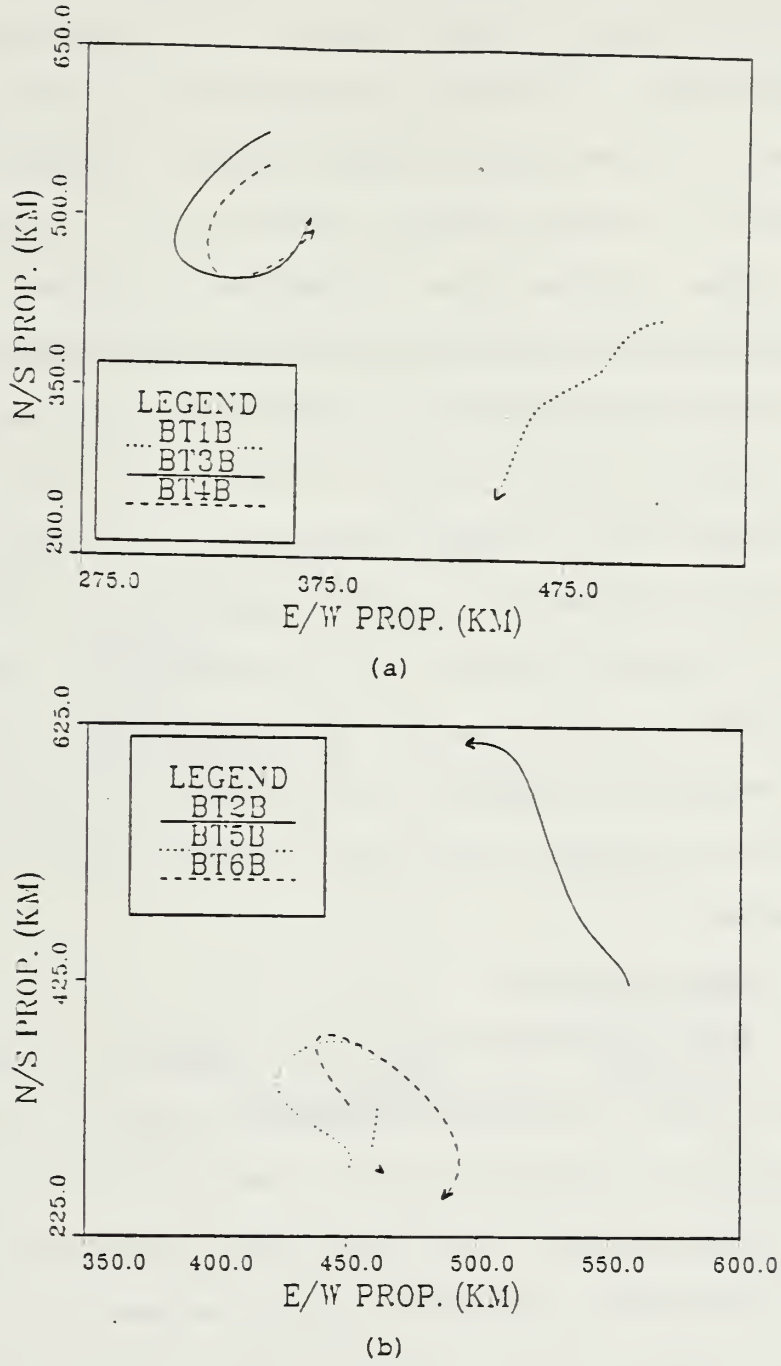

Figure 3.1 β Plane Vortex Trajectories (Opposite Sign Cases)

30 day trajectories for (a) anticyclones to the north of the jet with an isolated anticyclone reference (BT1β) and (b) cyclones to the south of the jet with an isolated cyclone reference (BT2β)

It is readily apparent from both Table 3 and Figure 3.1a that the jet has little influence initially on the ring in both the mid and far field cases. The initial propagations are southwest as in the no jet case. As the ring approaches the jet, propagation direction is reversed as the ring interacts with the jet. A similar phenomenon holds true for the zonal propagation tendencies with westward velocities being retarded as the ring approaches the jet and velocities being reversed to eastward as the ring comes into contact and interacts with the jet. The results here are mirrored duplications of the clockwise propagations of cyclones to the south of the jet as observed and described by Richardson (1980). The eddy motion in figure 3.1b does in fact resemble these observations to a large extent (see, for example, ring numbers 2, 3, 8 and 9 in Figure 1.4. The fact that Figures 3.1a and 3.1b are mirrored duplicates of each other exemplifies the symmetry of the dynamics of the eddy jet interaction.

3. Same Sign Cases

Figure 3.2 shows beta plane trajectories for simulations in which the sign of the ring velocity is the same as that of the shear vorticity on that side of the jet. Though these simulations are of a more hypothetical nature than the opposite sign cases discussed above, they are nonetheless included for comparison again with suggestions by Stern and Flierl (1987). They show that like sign point vortices are initially attracted to the jet while "winding" the jet interface around the vortex. The mutual influence tends to advect the ring downstream at speeds similar to that of the shear flow. The near

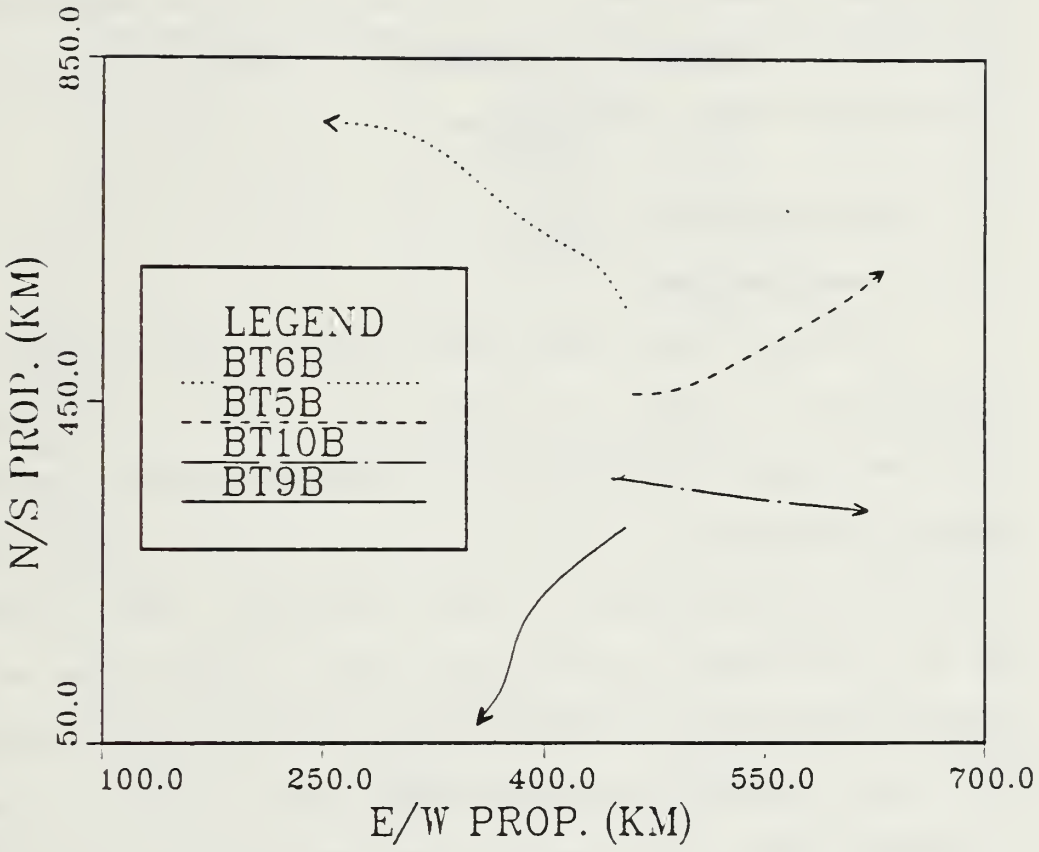

Figure 3.2 β Plane Vortex Trajectories (Same Sign Cases)

field cases in Figure 3.2 exhibit tendencies that agree qualitatively with their results. BT5β and BT9β on the other hand are initially displaced further from the jet and the nonlinear propagation tendencies overcome the influence of the jet and allow the rings to propagate at directions and speeds similar to that of the isolated ring cases discussed earlier. The eddy propagation associated with the eddy jet interaction (excluding beta effects) is more clearly illustrated in f plane experiments.

B. f PLANE EXPERIMENTS

1. Same Sign Cases

The same sign cases (BT71F, BT70F, BT65F and BT66F) have trajectories as shown in Figure 3.3. Without the countering influences of beta and nonlinear self advection the eddies are able to propagate downstream at rates as high as 30 km/day. These values are similar to those determined by Stern and Flierl. Minor differences are due to the finite radius of the eddy and width of the jet whose maximum speed is at its central axis. In the numerical simulations the, ring is unable to completely interact with the jet inner core as in the point vortex experiments by Stern and Flierl. Also of note is the initial attraction of the rings to the jet. This again is in agreement with Stern and Flierl. Experiments BT66F and BT71F (far field cases) did not run long enough to advect downstream as did the two near field cases, but of note is their eastward (downstream) turn at the latter stages of each run.

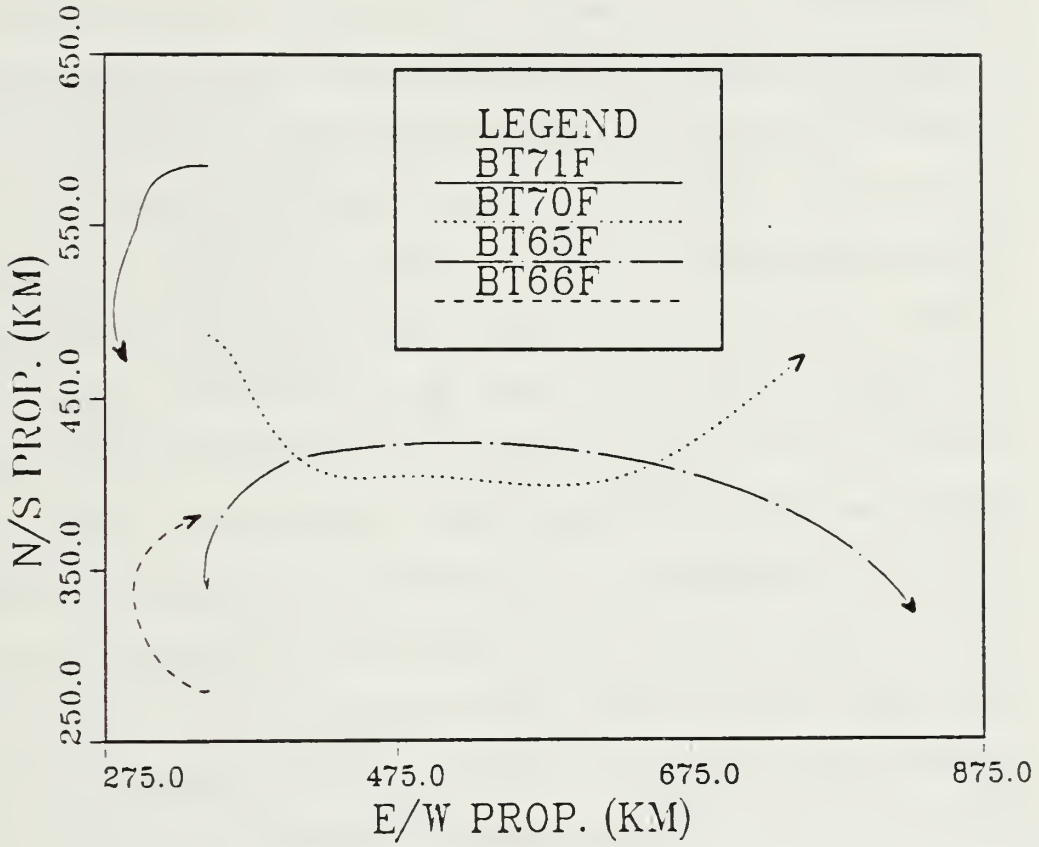

Figure 3.3 f Plane Vortex Trajectories (Same Sign Cases)

2. Opposite Sign Cases

The opposite vorticity sign f plane cases are the crux of this study. Beta induced westward motion (Mied and Lindemann, 1979) is thus eliminated as a propagation mechanisms. Meridional motion due to nonlinear effects, subsequent to Rossby dispersion induced distortions, is also removed. The southside f plane trajectories (as depicted in Figure 3.4) as well as all cases listed in Table 2, exhibit a propagation tendency and therefore a propagation mechanism that is not associated with the aforementioned mechanisms. Eddy propagation paths for these cases can be categorized as meridional and zonal. In the near field cases (small L(0)), the initial path is a meridional ejection away from the jet interface, followed by a westward drift. This response is particularly evident in the south side cases BT21F, BT38fF and BT34F. The motion for larger L(0) is a zonal motion, opposite to the jet direction (in this case westward).

Figure 3.5 shows the evolution of the potential vorticity in the upper layer for small L(0) experiment BT21F. This experiment exhibits the evolution of vorticity and is representative of all other experiments in this respect. As shown in Figure 3.4, this ring propagates initially perpendicular to the jet axis at 6.5 km/day. This southward motion is visibly less prominent as L(0) is increased in other experiments. The mechanism for this meridional motion is similar in nature to that of Stern and Flierl: close examination of the vorticity plots of Figure 3.5 depicts an entrapment of jet vorticity. The region between the southern edge of the jet and the eddy is one of strong anticyclonic shear. Anticyclonic relative

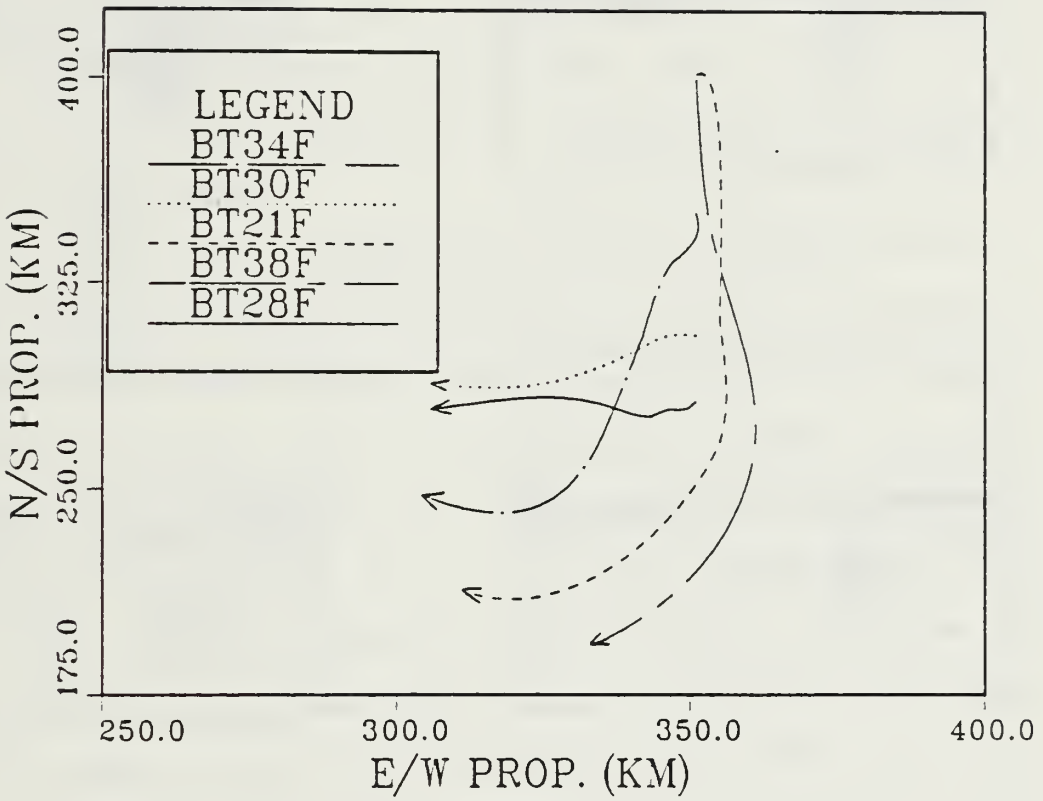

Figure 3.4 β Plane Vortex Trajectories (South Side Cyclones)

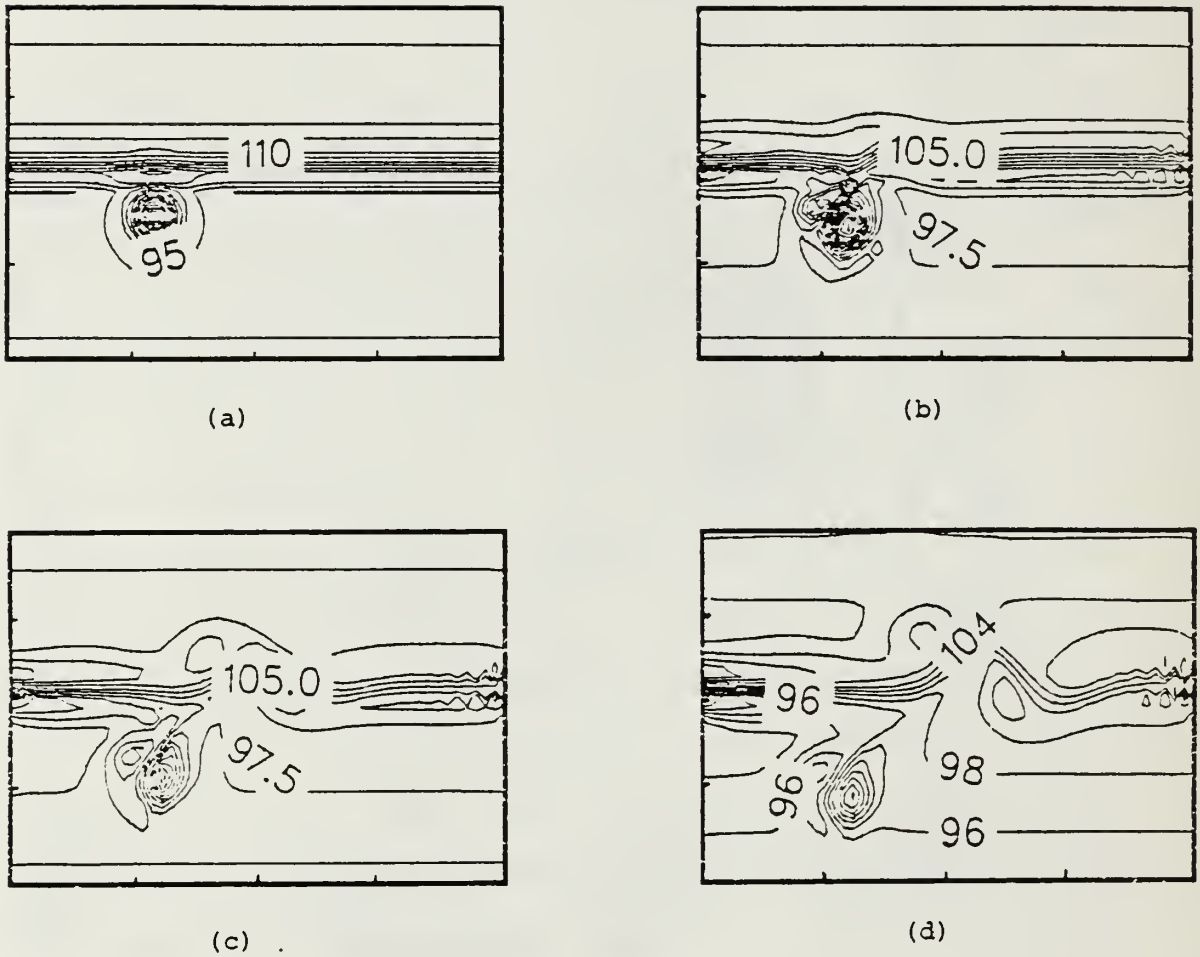

Figure 3.5 Evolution of Potential Vorticity for Experiment BT21F

Contours at (a) day 0, (b) day 6, (c) day 12 and (d) day 18

eddy is one of strong anticyclonic shear. Anticyclonic relative vorticity is then advected by the eddy away from the jet and is represented in this figure by a patch of anomalous anticyclonic vorticity to the west of the cyclone. The pairing of the anticyclonic and cyclonic vorticity results in a mutual advection/steering process that results in the initial southward propagation. A comparison of BT21F and BT38F also indicates that the pairing of eddy and jet vorticity occurs for stronger eddies and jets. BT21F has initial flow velocities of 50 cm/s in contrast to the remaining experiments in this study.

The jet/eddy interface and presence of this anomalous vorticity patch also results in a perturbation in the vortex azimuthal structure which further enhances this southward propagation. Figure 3.6 shows the velocity field of experiment BT34F on day 6. A strong azimuthal mode 1 perturbation exists with intensified gradients on the western side of the eddy. As the eddy weakens and propagates away from the jet axis, the anticyclonic vorticity patch is recaptured by the jet and is advected downstream by the jet, as in the like sign cases discussed previously. As it propagates and rotates to the north of the cyclone, the axis of the azimuthal mode 1 also rotates and the advection of the ring is thus turned to the west. Figure 3.7 shows the surface height field of near field experiment BT38F and exhibits this advection and rotation of the axis from day 6 to day 24.

Stern and Flierl attribute these tendencies to a "capture" of the jet interface by the eddy (Figure 3.8). Their results indicate the occurrence of this capture when the separation distance of the

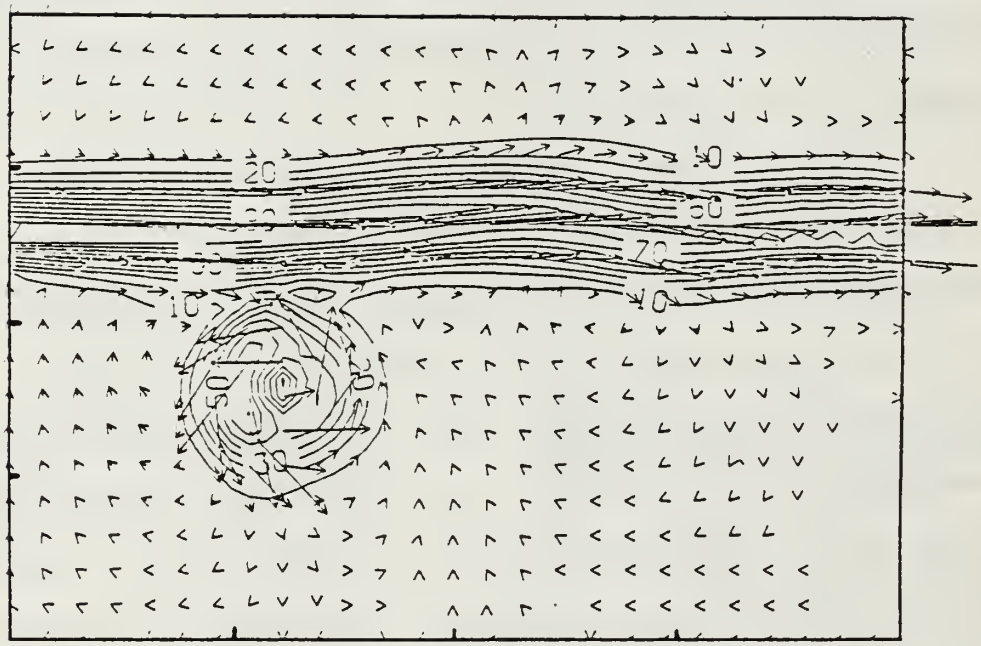

Figure 3.6 Velocity Field, Experiment BT34F on Day 6

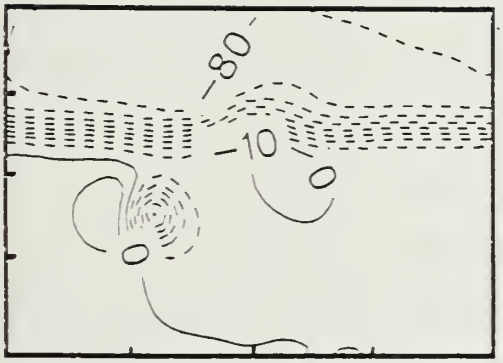

day 6

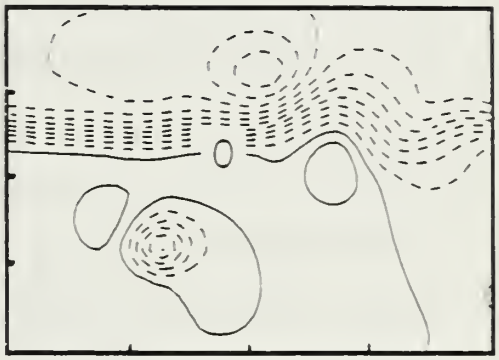

day 12

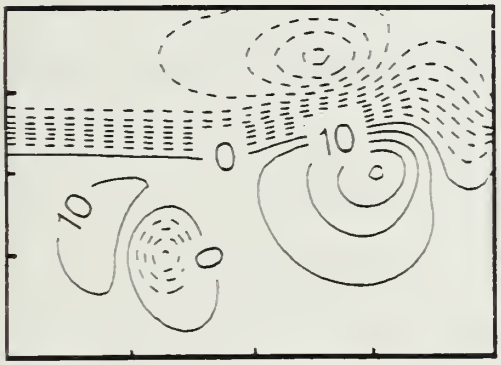

day 18

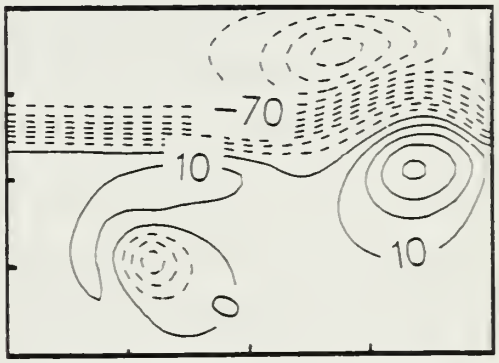

day 24

Figure 3.7 Height Anomaly Fields. Experiment BT38F

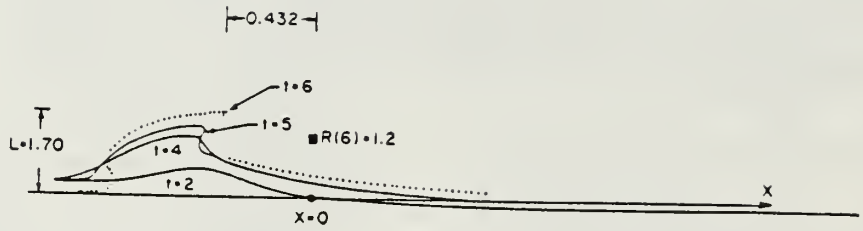

Figure 3.8 "Capture" of the Current Interface

"Capture" of the current by an anticyclonic vortex initially at R(0) = 0.5 and located at the indicated point R(6) = 1.2 at time t = 6. L(x, 6) is partially indicated by the solid circles, and the remaining three curves are for t = 5.4, and 2, respectively.

vorticity is then advected by the eddy away from the jet and is represented in this figure by a patch of anomalous anticyclonic vorticity to the west of the cyclone. The pairing of the anticyclonic and cyclonic vorticity results in a mutual advection/steering process that results in the initial southward propagation. A comparison of BT21F and BT38F also indicates that the pairing of eddy and jet vorticity occurs for stronger eddies and jets. BT21F has initial flow velocities of 50 cm/s in contrast to the remaining experiments in this study.

The jet/eddy interface and presence of this anomalous vorticity patch also results in a perturbation in the vortex azimuthal structure which further enhances this southward propagation. Figure 3.6 shows the velocity field of experiment BT34F on day 6. A strong azimuthal mode 1 perturbation exists with intensified gradients on the western side of the eddy. As the eddy weakens and propagates away from the jet axis, the anticyclonic vorticity patch is recaptured by the jet and is advected downstream by the jet, as in the like sign cases discussed previously. As it propagates and rotates to the north of the cyclone, the axis of the azimuthal mode 1 also rotates and the advection of the ring is thus turned to the west. Figure 3.7 shows the surface height field of near field experiment BT38F and exhibits this advection and rotation of the axis from day 6 to day 24.

Stern and Flierl attribute these tendencies to a "capture" of the jet interface by the eddy (Figure 3.8). Their results indicate the occurrence of this capture when the separation distance of the point vortex from the jet is less than a specified distance T (defined

as the square root of vortex circulation divided by the potential vorticity of the shear flow). For quantitative comparison the jet edge vorticity in this numerical study was estimated as $0.5 * 10^{-4} s^{-1}$. This value was also that of the eddy, due to its similar Gaussian structure. For the eddy radius here T = 71 km. Nondimensionalizing as in Stern and Flierl, R(0) = L(0)/T. Table 2 includes values for the R(0) used within this study.

For barotropic point vortices, Stern and Flierl show little meridional motion for $R(0) > 2.4$. The results of this study (Table 2) indicate meridional motion for $R(0) < 2.4$ which is substantially less for values greater than 2.4. These results are therefore in agreement with Stern and Flierl with respect to the distance within which nonlinear eddy/jet interactions and subsequent propagation occur.

Perturbation and orientation is also evident in mid to large R(0) experiments indicating that violent collisions and interactions between the eddy and jet are not necessary for this meridional motion to occur. Upper layer potential vorticity for R(0) = 1.6 (Figure 3.9) illustrates a weaker capture of vorticity from the jet than is evident in BT21F. Also evident in the height fields is the persistent orientation of the azimuthal mode 1 structure. Azimuthal mode 1 distortions associated with Rossby wave dispersion of eddies on a beta plane have been seen to lead to meridional vortex motion in nonlinear eddies. The distortion here is such that cyclone (anti-cyclone) self-advection to the south (north) is opposite to that of dispersion induced distortion.

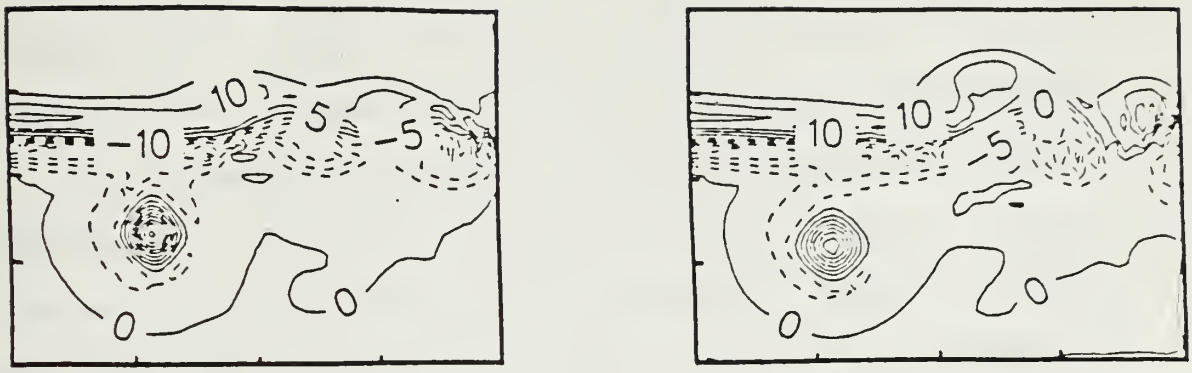

(a)

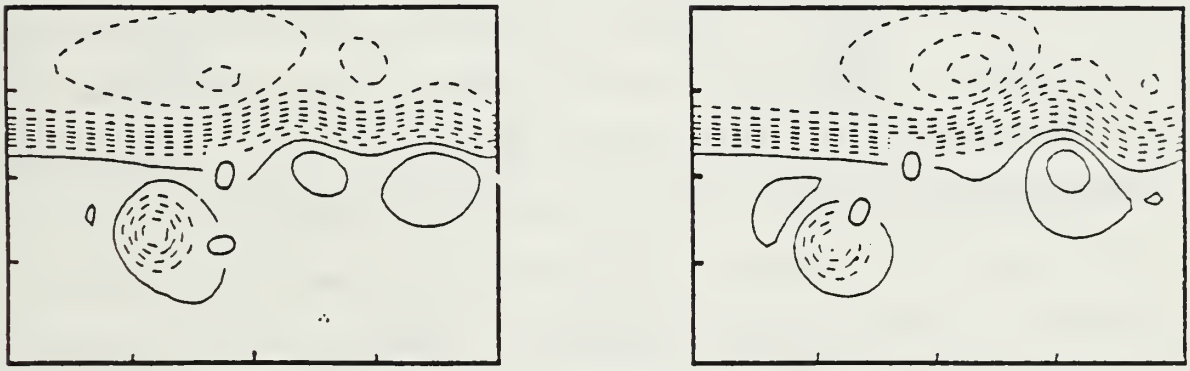

(b)

Figure 3.9 Experiment BT34F

Contours of upper layer (a) potential vorticity and (b) surface height anomaly

In addition to the meridional motions described above, Stern and Flierl also propose a theory of predominant antiparallel (zonal) propagation associated with the larger R(0) values. They suggest a westward motion related to linear vorticity dynamics in which the eddy induces a perturbation on the jet. The perturbation vorticity is opposite in sign to that of the vortex vorticity. The resulting vorticity anomaly interacts with the eddy, producing westward propagation. The larger separation distances prevent the more extensive nonlinear "capture" of the interface as previously described.

Experiment BT28F illustrates this nonlinear capture. A small perturbation is seen on the outer jet contours in Figure 3.10. The perturbation eventually advects downstream but imparts a westward propagation to the eddy. In this experiment the eddy averages 1.4 km/day westward motion. Stern and Flierl obtain a dimensional velocity of 12 km/day for the same initial separation conditions. Although this is a factor of 10 times greater than that determined in BT28F and other similar experiments, experiment BT28F is more in keeping with observational studies. Again this is attributed to the more realistic model representation of the Gulf Stream. It is also interesting to note that eddy azimuthal distortions seen in small L(0) do not occur in large L(0) experiments.

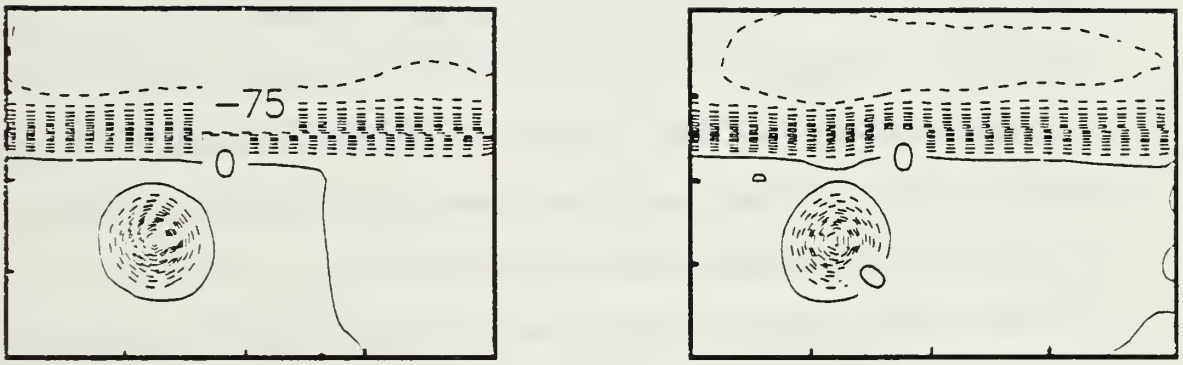

Figure 3.10 Height Anomaly Field, Experiment BT28F

Contours of height anomaly at (a) day 6, (b) day 12

IV. DISCUSSION AND CONCLUSIONS

A. JET INDUCED EDDY PROPAGATION TENDENCIES

Azimuthal perturbations to Gulf Stream rings have been observed in repeated hydrographic surveys of a ring as well as in satellite data. Hydrographic surveys indicate that a ring can undergo oscillations between axisymmetric mode 0 and mode 1 or mode 2 perturbations. Spence and Legeckis (1981) determined that a cyclonic ring was elliptical while interacting with the Gulf Stream, with its major-minor axis rotating with the mean flow of the vortex (cyclonically). The ring returned to circular (mode 0) when further from the stream. Numerous other studies have also shown this tendency to return to circular upon ring separation from the Stream.

This study indicates that a strong azimuthal mode 1 perturbation is induced on an isolated eddy by interaction with the jet when the eddy is initially close to the jet. The orientation is such that the eddy is intensified on the western side if R(0) is sufficiently small enough to "capture" shear vorticity from the same side of the jet. In this case the eddy vorticity pairs with this anomalous patch of opposite sign vorticity. The subsequent meridional motion is then due both to the western intensification of the ring and also to the mutual advection of the vortex pair.

As the vortex (in this case a cyclone to the south of the jet) moves away from the jet, the anticyclonic vorticity anomaly is advected zonally along the jet axis. This in turn rotates the axis of

the mode 1 vortex anticyclonically resulting in a north side intensification and westward motion. As vortex and jet separate completely, the vortex evolves through mode 2 to axisymmetric in a time scale consistent with the results of McCalpin (1987). Coincident with the evolution to axisymmetry is a decrease of the meridional and zonal propagation rates.

In larger R(0) experiments (>2.5), the initial interaction between jet and eddy is weaker and the mode 1 perturbation is absent. The eddy remains axisymmetric and interacts weakly with a perturbation induced on the edge of the jet. This results in predominantly zonal motion opposite to the stream direction.

B. EDDY COALESCENCE WITH A JET

Although the focus of this paper is not on the coalescence of an eddy with a jet, certain conditions appear necessary for coalescence to occur. The experiments here show no tendency for eddies to coalesce with the jet when the jet is in a stable zonal configuration. Instead, an eddy interaction with the jet allows the eddy to capture opposite sign shear vorticity associated with the jet edge, causing vortex pairing and eddy ejection from the jet.

Eddy interactions with an unstable jet can be rather different. Additional experimentation showed that eddies can coalesce with an unstable jet when a collision occurs between an eddy and a meander with vorticity of the same sign. Figure 4.1 shows experiment RG99 which illustrates a merger of a cyclone with a southward extending cyclonic meander. Coalescence occurs due to the comparable vorticity of eddy and meander. An experiment with an anticyclone in the same

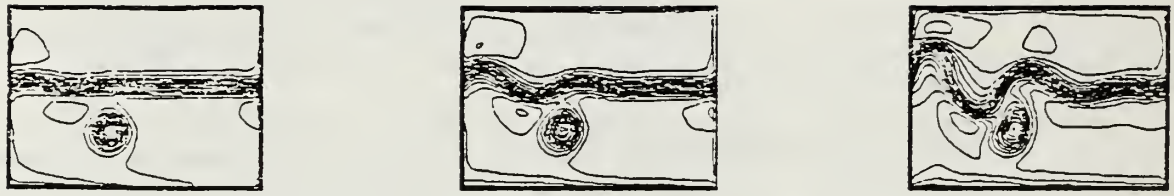

(a)

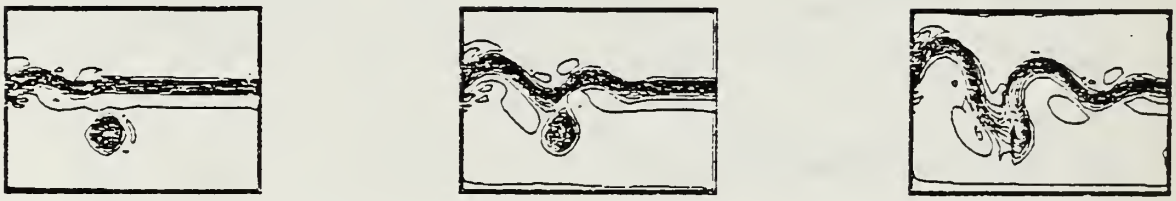

(b)

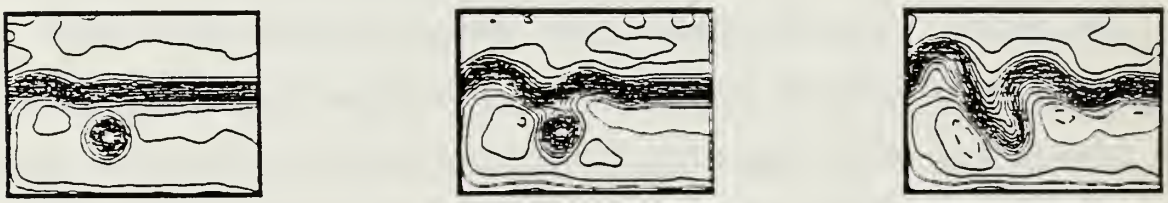

(c)

Figure 4.1 Experiment RG99β

Contours of (a) upper layer potential vorticity (b) lower layer potential vorticity and (c) height field

location did not indicate a merger, but instead the anticyclone advected rapidly eastward with the jet.

C. RECOMMENDATIONS FOR FUTURE STUDIES

This modeling work provides a base on which to build and further develop studies in this area that would better simulate the Gulf Stream eddy propagation. A first step would be the utilization of a baroclinically stable and then an unstable jet to further advance the solution of the actual jet induced eddy propagation tendencies. Next, imposing periodic inflow and outflow boundaries would enable for a reduction in the A_h lateral friction term and thus allow for longer experimental runs. A final step would be the implementation of real hydrographic and satellite data in the initialization of the model. If approached systematically as suggested here, this would eventually provide for real time eddy propagation and jet meander forecasting for operational usage in the USN.

D. CONCLUSIONS

The results of this study indicate that an isolated vortex interacting with a comparable strength stable jet can acquire a meridional propagation tendency away from the jet. The translational speed associated with eddy/jet interactions is dependent on the initial eddy/jet separation distance and the strength of the eddy and jet. For Gulf Stream velocities, the eddy translation speed away from the jet increases with decreasing eddy/jet separation if the initial separation distance is less than about 4 times the internal Rossby radius. For eddies initially within this distance from the

jet, the meridional speed is proportional to the strength of the eddy and jet. For eddies initially outside this range, westward propagation can occur which is associated with weaker eddy/jet interactions. The meridional and zonal propagation tendencies are related to vortex pairing between the eddy and opposite sign vorticity of the jet edge, as is found by Stern and Flierl (1987) where point vortices and a jump discontinuity jet were used. In strong interaction simulations, the motion is also associated with strong azimuthal mode 1 perturbations acquired by the eddy in the eddy/jet interaction. These experiments suggest that a strong ring cannot coalesce with a jet when the jet is in a stable configuration. In experiments where the jet is dynamically unstable however, coalescence is possible only when an eddy collides with a meander of like sign vorticity. In this case, the above propagation tendencies are no longer observed.

LIST OF REFERENCES

Camerlengo, A., and J.J. O'Brien, 1980: Open boundary conditions in rotating fluids. J. Comput. Phys., 35, 12-35.

Firing, E., and R.C. Beardsley, 1976: The behavior of a barotropic eddy on a β-plane. J. Phys. Oceanogr., 6, 57-65.

Flierl, G., 1977: The application of linear quasi-geostrophic dynamics to Gulf Stream rings. J. Phys. Oceanography, 7, 315-379.

Fuglister, F.C., 1972: Cyclonic rings formed by the Gulf Stream, 1965-66. Studies in Physical Oceanography, Vol. 1, Gordon and Breach, 137-167.

_____, 1977: A cyclonic ring formed by the Gulf Stream 1967. A Voyage of Discovery, Pergamon Press, 177-198.

Hurlburt, H., and J.D. Thompson, 1980: A numerical study of Loop Current intrusions and eddy shedding. J. Phys. Oceanogr., 9, 1611-1651.

_____, and _____, 1982: The dynamics of the Loop Current and shed eddies in a numerical model of the Gulf of Mexico. Hydrodynamics of Semi-Enclosed Seas, Elsevier, 243-298.

Iselin, C.O.D., 1936: A study of the circulation of the western North Atlantic, Pap. Phys. Oceanography Meteorol., 4, 101.

Lai, D.Y., and P.L. Richardson, 1977: Distribution and movement of Gulf Stream rings. J. Phys. Oceanogr., 7, 670-683.

McCalpin, J.D., 1987: On the adjustment of azimuthally perturbed vortices. J. Geophys. Res., 92, 8213-8225.

Mied, R.P. and G.J. Lindemann, 1979: The propagation and evolution of cyclonic Gulf Stream rings. J. Phys. Oceanogr., 9, 1183-1206.

Richardson, P.L., R.E. Cheney, and L.V. Worthington, 1978: A census of Gulf Stream rings, Spring 1975. J. Geophys. Res., 83, 6136-6144.

Richardson, P.K., 1980: Gulf Stream trajectories. J. Phys. Oceanogr., 10, 90-104.

Richardson, P.L., 1983: Gulf Stream rings. Eddies in Marine Science, Chap. 2, A. Robinson, Ed., Springer-Verlag.

Smith, D.C., IV, and R.O. Reid, 1982: A numerical study of non-frictional decay of mesoscale eddies. J. Phys. Oceanogr., 12, 244-255.

_____, and J.J. O'Brien, 1983: The interaction of a two layer isolated mesoscale eddy with topography. J. Phys. Oceanogr., 13, 1681-1697.

_____, 1986: A numerical study of Loop Current eddy interaction with topography in the western Gulf of Mexico. J. Phys. Oceanogr., 16, 1260-1272.

Spence, T.W. and R. Legeckis, 1981: Satellite and hydrographic observation of low-frequency wave motions associated with a cold core Gulf Stream ring. J. Geophys. Res., 86, 1945-1953.

Stern, M.E. and G.R. Flierl, 1987: On the interaction of a vortex with a shear flow. J. Geophys Res., 92, 10733-10744.

Warren, B.A., 1967: Notes on translatory movement of rings of current with application to Gulf Stream eddies. Deep-Sea Res., 14, 505-524.

Watts, D.R., 1983: Gulf Stream variability. Eddies in Marine Science, Chap. 6, A. Robinson, Ed., Springer-Verlag.

Worthington, L.V., 1976: On the North Atlantic Circulation. The Johns Hopkins Oceanogr. Study No. 6, Johns Hopkins Univ. Press, Baltimore. 110 pp.

INITIAL DISTRIBUTION LIST

		No. Copies
1.	Defense Technical Information Center Cameron Station Alexandria, VA 22304-6145	2
2.	Library, Code 0142 Naval Postgraduate School Monterey, CA 93943-5002	2
3.	Chairman (Code 68Co) Department of Oceanography Naval Postgraduate School Monterey, CA 93943-5100	1
4.	Chairman (Code 63Rd) Department of Meteorology Naval Postgraduate School Monterey, CA 93943-5100	1
5.	Prof. D. C. Smith, IV (Code 68Si) Department of Oceanography Naval Postgraduate School Monterey, CA 93943-5100	3
6.	Prof. A. J. Semtner, Jr., (Code 63Se) Department of Oceanography Naval Postgraduate School Monterey, CA 93943-5100	1
7.	Director Naval Oceanography Division Naval Observatory 34th and Massachusetts Avenue NW Washington, DC 20390	1
8.	Commander Naval Oceanography Command NSTL Station Bay St. Louis, MS 39522	1
9.	Commanding Officer Naval Oceanographic Office NSTL Station Bay St. Louis, MS 39522	1

10. Commanding Officer 1
Fleet Numerical Oceanography Center
Monterey, CA 93943

11. Commanding Officer 1
Naval Ocean Research and Development Activity
NSTL Station
Bay St. Louis, MS 39522

12. Commanding Officer 1
Naval Environmental Prediction Research Facility
Monterey, CA 93943

13. Chairman, Oceanography Department 1
U.S. Naval Academy
Annapolis, MD 21402

14. Chief of Naval Research 1
800 North Quincy Street
Arlington, VA 22217

15. Office of Naval Research (Code 420) 1
Naval Ocean Research and Development Activity
800 North Quincy Street
Arlington, VA 22271

16. Scientific Liaison Office 1
Office of Naval Research
Scripps Insitution of Oceanography
La Jolla, CA 92037

17. Chief, Ocean Services Division 1
National Oceanic and Atmospheric
Administration
8060 Thirteenth St.
Silver Spring, MD 29010

18. Commanding Officer 1
Naval Eastern Oceanography Center
Naval Air Station
Norfolk, VA 23511

19. Commanding Officer 1
Naval Oceanography Command Center
Box 31
FPO New York, NY 09540-3200

20. Program Director 1
Physical Oceanography
National Science Foundation
Washington, DC 20550

21. Dr. C. N. K. Mooers, Director — 1
Institute for Naval Oceanography
Bldg. 1100, room 311
NSTL Station
Bay St. Louis, MS 39529

22. Director of Research Administration — 1
Code 012
Naval Postgraduate School
Monterey, CA 93943

23. Officer in Charge — 1
Naval Oceanography Command Detachment
APO New York 09406-5000

24. LT George P. Davis, Jr. — 3
P.O. Box 806
Grifton, NC 28530

Thesis
D169595 Davis
c.1 A numerical study of eddy interactions with a barotropic oceanic jet.